Structure-dependent bypass of DNA interstrand crosslinks by translesion synthesis polymerases

The Vinh Ho[1], Angelo Guainazzi[1], Semsi Burak Derkunt[1], Milica Enoiu[2] and
Orlando D. Schärer[1,3,*]

[1]Department of Pharmacological Sciences, Stony Brook University, Stony Brook, NY 11794-3400, USA,
[2]Institute of Molecular Cancer Research, University of Zurich, 8057 Zurich, Switzerland and [3]Department of
Chemistry, Stony Brook University, Stony Brook, NY 11794-3400, USA

ABSTRACT

DNA interstrand crosslinks (ICLs), inhibit DNA metabolism by covalently linking two strands of DNA and are formed by antitumor agents such as cisplatin and nitrogen mustards. Multiple complex repair pathways of ICLs exist in humans that share translesion synthesis (TLS) past a partially processed ICL as a common step. We have generated site-specific major groove ICLs and studied the ability of Y-family polymerases and Pol ζ to bypass ICLs that induce different degrees of distortion in DNA. Two main factors influenced the efficiency of ICL bypass: the length of the dsDNA flanking the ICL and the length of the crosslink bridging two bases. Our study shows that ICLs can readily be bypassed by TLS polymerases if they are appropriately processed and that the structure of the ICL influences which polymerases are able to read through it.

INTRODUCTION

Bifunctional chemical agents such as cisplatin (CP) or nitrogen mustards (NMs) are highly cytotoxic due to their ability to form DNA interstrand crosslinks (ICLs) and are commonly used in cancer chemotherapy. ICLs render the two strand of a DNA helix inseparable, and thereby inhibit transient division of the two strands, providing a complete block to DNA replication and transcription (1,2). ICLs can also be induced by endogenous agents such as aldehydes formed by lipid peroxidation (3), providing an evolutionary incentive for cellular ICL repair mechanisms. Although DNA ICLs are often considered as one class of DNA damage, they are structurally diverse, possibly requiring multiple cellular mechanisms to rid genomes of these lesions.

ICL repair has been genetically linked to factors of multiple DNA repair pathways, including those involved in nucleotide excision repair (NER), homologous recombination (HR) and translesion synthesis (TLS). ICL repair additionally involves the activity of a number of nucleases and the Fanconi Anemia pathway [reviewed in (4,5)]. How these factors mechanistically work together to remove ICLs is still poorly understood. Currently, ICL repair is believed to occur by at least two pathways (see Supplementary Figure S1 for current ICL repair models); one operating in the S-Phase triggered by the stalling of a replication fork at an ICL, and one outside of S-phase that may be initiated by NER or a stalled RNA polymerase (6). Common features of both pathways include an endonucleolytic unhooking step that releases the ICL from one of the two strands of the duplex, and a TLS step that bypasses the unhooked ICL and restores one of the two strands, providing one intact template to complete the repair process (Supplementary Figure S1).

At least 15 DNA polymerases are known in eukaryotes and many of those have the ability to bypass a number of structurally diverse lesions, and are therefore candidates for the bypass of ICLs (7,8). There is strong genetic (9–13) and biochemical (14) evidence for a key role for Pol ζ in ICL repair, as cells deficient in Pol ζ display the most pronounced hypersensitivity to ICL forming agents. Pol ζ is a heterodimeric B-family polymerase, consisting of the catalytic subunit Rev3 and the accessory subunit Rev7 and has the ability to bypass certain DNA lesions [reviewed in (15,16)].

A second polymerase, Rev1, a Y-family polymerase, is epistatic to Pol ζ for ICL repair (13,17,18). Rev1 has an atypical template-dependent deoxycytidyl transferase activity (19–21). Rev1 and Pol ζ can cooperate to bypass certain DNA damages and it has been suggested that they may do so in the context of ICL repair (12,14,22).

To what extent other polymerases with the ability to bypass various DNA lesions are involved in ICL repair is less clear-cut. Human XP-V cells, which lack Pol η, were shown to be moderately hypersensitive to ICL-forming agents CP and psoralen (23–25) and are

*To whom correspondence should be addressed. Tel: +1 631 632 7545; Fax: +1 631 632 7546; Email: orlando@pharm.stonybrook.edu

partially defective in reactivating a gene in a reporter plasmid containing a mitomycin C ICL (26), indicating a possible role for Pol η in ICL repair at least for certain lesions. More recently, biochemical and cellular studies have strongly implicated Pol κ in the repair of minor groove ICLs, such as those formed by mitomycin C and bifunctional dialdehydes that are formed by lipid peroxidation (27). Pol ν, in contrast, exhibits a strong preference for bypassing major groove lesions, including ICLs (28).

Since TLS polymerases bypass structurally distinct DNA lesions with various efficiencies [reviewed in (7,8,15)] and ICLs induced by various agents are structurally heterogeneous (1,2), the requirement of individual polymerases to bypass ICLs likely also depends on the structural features of various ICLs.

In this study, we took advantage of the ability of our laboratory to generate a series of major groove ICLs that induce various degrees of distortion in the DNA helix (29,30) to systematically investigate how structural variation affects the activity of TLS polymerases. We found that two factors greatly affect the efficiency of lesion bypass: the amount of dsDNA flanking an ICL and the length of the ICL linker between the two crosslinked guanosine residues. Our studies show that major groove ICLs can be bypassed by a number of TLS polymerases and that the efficiency of this reaction is dramatically affected by the structural features of the ICL.

MATERIAL AND METHODS

Preparation of CP ICL templates

High pressure liquid chromatography (HPLC) purified oligonucleotides for cisplatination were purchased from Integrated DNA Technologies Incorporation. CP was purchased from Sigma-Aldrich. Templates containing a defined CP ICL were prepared according to Hofr *et al.*

(31). A 20-mer containing one single guanine (Figure 1D, upper strand of CP1) at 125 μM concentration was reacted with 3-fold excess of monoaquamonochloro CP in 10 mM NaClO$_4$ pH 5.2 for 12 min at 37°C. The monoaquamonochloro CP was generated by precipitating chlorine with 0.9 molar equivalents of AgNO$_3$. The monoadduct was purified on a Mono Q 5/50 GL column (GE Healthcare) using a gradient from 0.1 to 0.8 M NaCl in 10 mM Tris–HCl pH 7.4. Monoadducts were then annealed to a complementary 39-mer (Figure 1D) and crosslink formation was promoted by exchanging the buffer to 100 mM NaClO$_4$ pH 5.2. The crosslinked oligonucleotides were purified under denaturing conditions (10 mM NaOH) on a Mono Q 5/50 GL column (GE Healthcare) with a gradient from 0.1 M to 0.8 M NaCl. Amicon Ultra-4 Centrifugal Filters (3000 NWML) were used to exchange buffer (10 mM Tris–HCl pH 7.5, 10 mM NaClO$_4$) and to concentrate the crosslinked oligonucleotides.

For the trimmed templates, the upper strand of CP1 contained deoxyuracil residues at the indicated sites (Figure 1D). Purified crosslinked products of 600 pmol were first treated with excess amount (10 U) of uracil DNA glycoslase (New England Biolabs) for 10 min at 37°C to generate abasic sites at the uracils, and then incubated with 100 mM NaOH in a total volume of 60 μl at room temperature for 2 h to cleave the abasic sites. The reaction was neutralized by adding 6 μl of 1 M acetic acid and the buffer was exchanged to 10 mM Tris–HCl pH 8.0, 1 mM EDTA using Amicon Ultra-4 Centrifugal Filters (3000 NWML).

To analyze the crosslinked oligonucleotides, they were 5′-labeled by T4 polynucleotide kinase with γ-[^{32}P]-dATP and analyzed on a 10% denaturing polyacrylamide gel (7 M Urea). The gel was dried and exposed to phosphor imager screens and bands visualized on a Typhoon 9400 (GE Healthcare).
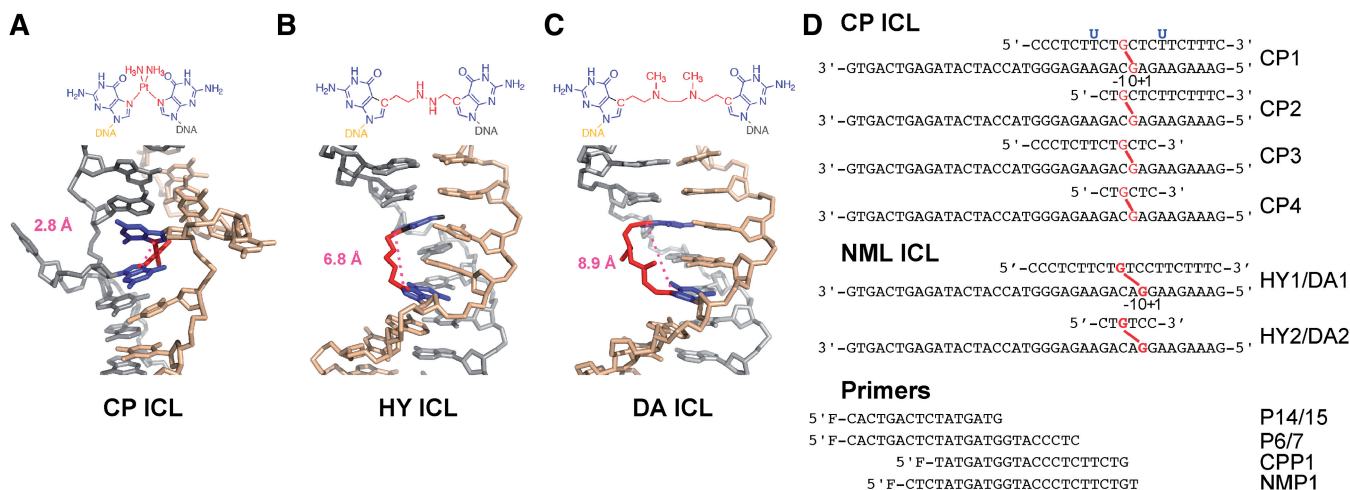

Figure 1. Structure and sequence of TLS polymerase templates. Chemical and 3D structure of the CP (CP ICL, **A**), HY (HY ICL, **B**) and DA (DA ICL, **C**) ICLs. The crosslinked bases are highlighted in blue, the ICL bridge in red. The distance spanning the two crosslinked dG residue is indicated in magenta, highlighting the different degrees of distortion induced by the three ICLs. The DNA structures were generated using PYMOL, using the coordinates 1DDP (A), models generated by molecular modelling in Ref 30 (B); and modelling of the ICL into B-form DNA (C). (**D**) Sequence of the crosslinked oligonucleotides with the location of the CP, HY and DA ICL highlighted in red. The position of the uracil residues used to generate the resected templates (CP2-4, HY2 and DA2) by treatment with UDG and NaOH are indicated in blue. Primers were labeled 5′ with either 6-FAM or HEX fluorophores. The positions are marked as 0 at, minus before and plus after the position of the crosslinked base on the template strand.

Preparation of nitrogen mustard mimic ICL templates

The template containing a NML ICLs were prepared as described in Angelov *et al.* and Guainazzi *et al.* (29,30). To obtain the trimmed templates the same method was used as with the CP ICL templates. The crosslinked oligonucleotides were analyzed by 5′ labeling with T4 polynucleotide kinase and γ-[^{32}P]-ATP and electrophoresis on a 15% denaturing polyacrylamide gel. The dried gels were exposed to phosphor imager screens and bands visualized on a Typhoon 9400 (GE Healthcare).

Enzymes

Human Pol η (with C-terminal His tag, purified from insect cells) and Pol ι (with N-terminal GST tag) were a gift from Drs Ekatarina Frank and Roger Woodgate (NIH) (32). Human Pol κ [with N-terminal His tag (33)] and *Saccharomyces cerevisiae* (*S. cerevisiae*) Pol ζ [with N-terminal His tags on the N-termini of the Rev3 and Rev7 subunits (33)] and Rev1 [with N-terminal His tag (20)] were purchased from Enzymax.

Polymerase assays

The templates were annealed to 6-FAM or HEX labeled primers wtih a primer to template ratio of 1:2–1:3 in annealing buffer (10 mM Tris–HCl pH 8.0, 50 mM NaCl). To avoid decrosslinking, annealing was performed at room temperature over night. The annealing reaction was checked on a native 20% polyacrylamide gel (data not shown). For the strand displacement control substrate, primer, template and downstream strand were annealed in a 1:2:5 ratio.

The primer extension reactions were performed in 10 μl volume, containing 5 nM primer–template with respect to the primer and 100 μM dNTPs. Reaction buffer for Pol κ, Pol ι and Pol η contained: 40 mM Tris–HCl pH 8.0, 0.1 mg/ml bovine serum albumin, 10 mM dithiothreitol and 2.5% glycerol (32). Pol κ and Pol η reactions contained 5 mM and 250 μM MgCl$_2$, respectively, Pol ι reactions contained 100 μM MnCl$_2$, in accordance with published procedures (32). The concentrations used for the polymerases were as follows: Pol κ 0.2 nM, 2 nM and 20 nM; Pol ι and Pol η: 4 nM, 40 nM and 400 nM.

Reaction buffer for Pol ζ and Rev1 contained 25 mM potassium phosphate pH 7.0, 0.1 mg/ml BSA, 25 mM dithiothreitol, 5 mM MgCl$_2$ and 5% glycerol (34). The concentration of Pol ζ in the reaction was 0.4, 4 and 35 nM. Rev1 concentration was at 40 nM. Reaction containing Pol ζ and Rev 1 as complex were at 20 nM. Standard reaction time was 10 min for all polymerases used. For all insertion reactions, the highest enzyme concentration was used.

The reactions were stopped by adding an equal amount of formamide loading buffer (80% formamide, 1 mM EDTA) and heated up to 95°C for 3–4 min. The extension products were separated on an 8–10% 7 M urea polyacrylamide gel. The fluorescence of the labeled primer was detected using a Typhoon 9400 (GE Healthcare).

RESULTS

Preparation of major groove cisplatin and nitrogen mustard ICL templates for primer extension studies

Previous investigations of lesion bypass of ICLs have used psoralen and dialdehyde substrates, which form adducts between the bases or in the minor groove (2). In contrast, ICLs formed by CP and NMs, the two most commonly used ICL-forming agents in antitumor therapy, react preferentially with the N7 position of guanine forming a bridge in the major groove of DNA (Figure 1A). CP preferentially reacts with two guanines in a GC sequence (35), while NMs prefer a GNC sequence (36–38). The two ICLs affect the structure of the DNA duplex in distinct ways: a CP ICL unwinds the DNA by 70° and forces the two cytosines that pair with the crosslinked guanines out of the double helix, relocating the N7 position of the guanines to the minor groove and introducing a high degree of helix distortion (Figure 1A) (39,40). By contrast, NM ICLs and a stable mimic (HY ICL), recently synthesized in our laboratory (29,30), only introduce a minor bend into the helix and retain mostly B-form DNA (Figure 1B) (38,41). Furthermore, our synthetic approach allowed for the synthesis of nitrogen mustard-like ICLs (NML ICLs) in which the length of the bridge between the crosslinked guanines is increased, resulting in an ICL that we predict to be free of any distortion (Figure 1C). The availability of these substrates allowed us to study systematically how major groove ICLs affect TLS.

The CP ICL-containing template CP1 was prepared (Figure 1D) following a published procedure by Hofr *et al.* (31) between a 20- and 39-mer generating a double-stranded crosslinked oligonucleotide with a 3′-overhang, which was determined to be >93% pure following ion exchange purification (Supplementary Figure S2A, lanes 1, 3 and 5).

The NML ICLs (Figure 1B and C) were prepared according to a procedures established in our laboratory (29,30). A 20-mer containing 7-deazaguanosine functionalized with an acetaldehyde group and a 39-mer functionalized with either formyl aldehyde or another acetaldehyde group were annealed and crosslinked by reductive amination with hydrazine (HY) or dimethylethylendiamine (DA), respectively. The crosslinked templates were purified by denaturing polyacrylamide gel electrophoresis (PAGE) yielding HY1 and DA1, respectively. Both substrates have a purity of >95% (Supplementary Figure 2B, lanes 1 and 3).

CP1, HY1 and DA1 were annealed to a fluorescently labeled primer, P14/15, which leaves a three nucleotide gap to the crosslinked strand, and 14 and 15 nt to the crosslinked base on the template strand, respectively. We tested these substrates with Klenow(-exo) fragment and found that this polymerase stalled 1 nt before the ICL on the template strand confirming the presence of an ICL at the predicted site (Supplementary Figure S3).

Since it was shown that resection of the crosslinked strand was beneficial for TLS by Pol κ (27), we further prepared templates in which the amount of dsDNA next to the ICL was shortened on the 5′, 3′ or both sides

(Figure 1D) by incorporating uracils instead of thymines into the 20-mer at specific sites. After treating these crosslinked oligonucleotides with uracil–DNA glycosylase and cleaving the generated abasic site under alkaline condition, we could form CP2, CP3, CP4, HY2 and DA2 oligonucleotides (Figure 1D) with >90% purity (Supplementary Figure S2).

Insertion opposite CP ICL by Y-family polymerases

In a first set of experiments, we tested the activity of a variety of polymerases on the CP1 substrate. An analogous duplex without an ICL was used as a control to monitor strand displacement synthesis. Incubation of Pol ζ with the non-crosslinked control substrate revealed that the polymerase stalled upon encountering the beginning of the duplex, but was able to displace the downstream strand at the highest concentration used (35 nM, Figure 2A, lane 3). The primer was extended until 2 nt before the end of the template strand, in agreement with previous results (42).

On the CP1 substrate, the p14/15 primer was extended until 1 nt before the adducted guanine (Figure 2A, lane 6), which we will refer to as −1 position (Figure 1D). Thus, Pol ζ was able to displace the crosslinked strand and polymerize up to the CP ICL, but failed to insert a nucleotide opposite the adducted guanine.

The Y-family polymerases, Pol κ, Pol ι and Pol η, were able to perform strand displacement synthesis on the control substrate with various degrees of efficiency (Figure 2B–D, compare lane 3). Surprisingly, Pol κ, Pol ι and Pol η were able to extend the primer on CP1 one step further than Pol ζ and stalled at 0 position, having inserted a dNTP opposite the crosslinked guanine (Figure 2B–D, lane 6). These results indicate that the insertion of a dNTP opposite a CP ICL can be accomplished by multiple polymerases.

Trimming of the DNA around the ICL facilitates insertion and bypass

Next, we wanted to investigate to what extent the 9–10 nt of dsDNA flanking the CP ICL on either side,
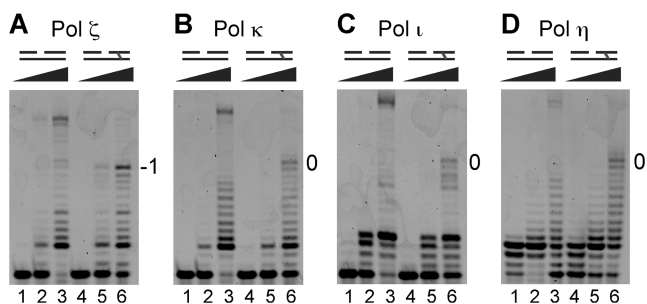
necessitating the strand displacement reaction, was responsible for the limited bypass (Figures 1 and 3). We reasoned that reducing the amount of dsDNA around the ICL might facilitate lesion bypass as previously shown by Minko *et al.* (27). We tested the activity of the polymerases on substrates having 3 nt 5′ to the ICL (CP2), 2 nt 3′ to the ICL (CP3) or with the duplex shortened on both sides of the ICL (CP4) (Figure 1D) with the ICL embedded in a duplex of 6 nt. These substrates were annealed to primers P14/15 and P6/7, leaving a 3 and 2 nt gap, respectively, and the ability of the polymerases to bypass these resected substrates was examined.

Resection of the duplex 5′ and 3′ to the ICL did not improve bypass by Pol ζ and stalling occurred at −1 position as we observed for the full-length ICL (Figure 3A, lanes 1–6). However, resection on both sides of the ICL (CP4), allowed for some insertion opposite the ICL and bypass, while −1 position was still the major stalling point (Figure 3A, lane 9). The insertion and bypass products accounted together for ~18% of all extension products, significantly more than the uncrosslinked impurity in CP ICL preparation in CP4 (~4%).
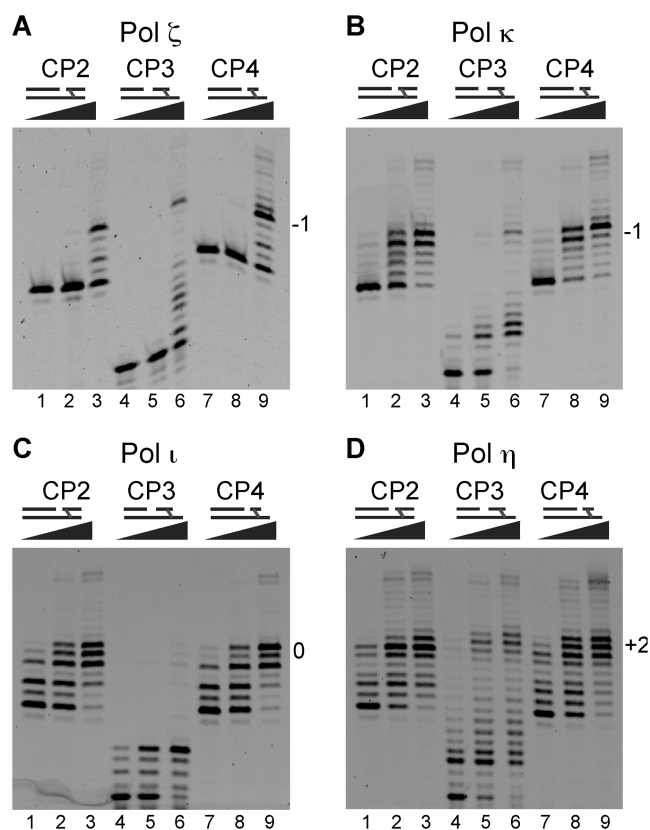

Figure 3. Resection of CP ICL templates facilitate partial lesion bypass. Templates with 5′-resected (CP2, lanes 1–3), 3′-resected (CP3, lanes 4–6) and 5′-3′-resected ends (CP4, lanes 7–9) were incubated with primer P6 (CP2, CP4) or P14 (CP3) and increasing amounts of (**A**) Pol ζ (0.4, 4, 35 nM), (**B**) Pol κ (0.2, 2, 20 nM), (**C**) Pol ι (4, 40, 400 nM) and (**D**) Pol η (4, 40, 400 nM). The position of the main stalling points is indicated at the right side of the gels. Note that Pol η can advance to +2 position on the templates with 3′-resection.

Figure 2. Primer extension reaction of CP ICL-containing template with Pol ζ, Pol κ, Pol ι and Pol η. Non-crosslinked template (lanes 1–3) and CP crosslinked template (CP1, lanes 4–6) were incubated with primer P14 and increasing amounts of (**A**) Pol ζ (0.4, 4, 35 nM), (**B**) Pol κ (0.2, 2, 20 nM), (**C**) Pol ι (4, 40, 400 nM) and (**D**) Pol η (4, 40, 400 nM) Pol ζ stalls at −1 position before the insertion opposite to the adducted guanine. Pol κ, Pol ι and Pol η stall at 0 position after inserting a nucleotide opposite to the adducted guanine.

Extension to the CP ICL by Pol κ was facilitated by 5′-resection (Figure 3B, lanes 1–3 and 7–9). Curiously, in contrast to the CP1 template, Pol κ mainly stalled at −1 position on all resected templates (Figure 3B, lanes 1–9). We have no explanation for this observation. Apparently the resection of the CP ICL leads to a structure that is not a good fit for the Pol κ active site. However, with the CP4 template we observed a small amount of insertion and bypass product in the range of Pol ζ.

5′-Resection also markedly facilitated the approach of Pol ι to the CP ICL (Figure 3C, lanes 1–3), but additional 3′-resection did not result in bypass of the lesion (Figure 3C, lanes 7–9). Extension by Pol ι on all resected templates stalled at 0 position after inserting a dNTP opposite the crosslinked guanine, similar to what was observed with the fully double-stranded CP1 substrate (Figure 2).

In contrast to the moderate effect of dsDNA resection around the CP ICL observed for Pol ζ, Pol κ and Pol ι, the shortening of the dsDNA around the ICL dramatically altered the ability of Pol η to insert a dNTP opposite the CP ICL and to bypass it. Even 3′-end resection allowed Pol η to reach +2 site, indicating complete bypass of the CP ICL (Figure 3D, lanes 4–6). The major stalling site on CP4 template was +2 position (22% of extension products; Figure 3D, lane 9), suggesting that Pol η could efficiently bypass CP ICL when the duplex around the ICL is reduced to 6 nt, but that extension to the full-length product was still limited to 11% of the total extension products.

These studies show that the resection of the duplex around the CP ICL facilitates insertion opposite the adducted guanine for all the polymerases tested, and in the case of Pol η greatly facilitate bypass to the +2 position.

Pol ζ is unable to extend insertion products by Rev1 under our experimental conditions

Rev1 cooperates with Pol ζ in the bypass of certain bulky DNA adducts (22,43) and we therefore tested if a complex of Rev1/Pol ζ would be more proficient in bypassing a CP ICL than Pol ζ alone. Since CP forms ICLs between two guanines, we hypothesized that Rev1 might be able to use its dCTP insertion activity followed by an extension of the insertion product by Pol ζ (44). However, the extension reaction with a Pol ζ/Rev1 complex did not result in more bypass product compared to Pol ζ alone (compare Figure 2 with Supplementary Figure S4) and the complex also stalled at −1 position (Supplementary Figure S4, lanes 1–9). Apparently, and consistent with previous observations (27), Pol ζ and Rev1 fail to work together productively under our experimental conditions.

Pol ζ and Rev1, but not other polymerases, have a preference for inserting a dCTP opposite a CP ICL

Since all polymerases tested were able to insert a dNTP opposite on the CP4 substrate to some degree, we wanted to determine the accuracy of insertion opposite the adducted guanine. Therefore, we carried out single nucleotide incorporation experiments by annealing the CP4 to the CPP1 primer (Figure 1D) and monitoring the

incorporation of the individual dNTPs by the different polymerases. Pol ζ inserted dCMP, but none of the other dNTPs, opposite the crosslinked guanine (Figure 4A), indicating that the enzyme accurately inserted a dCMP opposite a CP ICL. Rev1 also specifically incorporated dCMP opposite the CP ICL, in agreement with the reported deoxycytidyl transferase activity of Rev1 (19,45). However, the insertion opposite the crosslinked guanine was very inefficient (Figure 4B). A complex of Pol ζ/Rev1 gave the same result as Pol ζ alone (Figure 4C) indicating that most of the activity comes from Pol ζ.

The Y-family polymerases proved to be promiscuous in terms of inserting deoxynucleotides opposite the crosslinked guanine (Figure 4D–F). These polymerases are known to be highly error prone (46–48), in particular for certain lesions, and it is possible that the error frequency is even higher under the conditions in our experiments that allowed for bypass of the ICLs. We found that they were able to insert any of the individual dNTPs opposite the CP ICL. Even Pol κ, which is known to be the most accurate polymerase in the Y-family (49), inserted any of the dNTPs opposite the adducted guanine. Interestingly, both the insertion and first extension step by Pol η were highly inaccurate and all dNTPs were incorporated with similar efficiency at the 0 and +1 position (Figure 4). Overall, the insertion efficiencies with all polymerases tested were rather low, considering the high enzyme to substrate ratios.

The ICL bridge length influences the ability of polymerases to bypass NML ICLs

Having shown that bypass of highly distorting CP ICLs is possible after resection of the dsDNA around the ICL, we
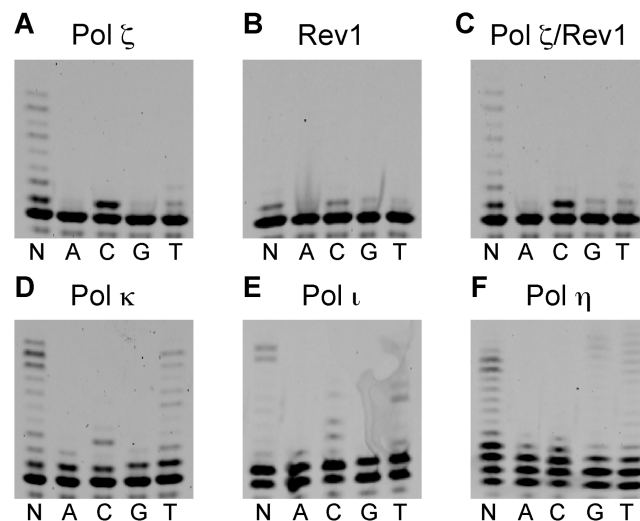

Figure 4. Pol ζ and Rev1, but not other Y-family polymerases accurately insert a single nucleotide opposite a CP ICL. The CP4 template was annealed to the CPP1 primer in presence of the indicated dNTPs and incubated with (**A**) Pol ζ (35 nM), (**B**) Rev1 (40 nM), (**C**) Pol ζ/Rev1 (20 nM each), (**D**) Pol κ (20 nM), (**E**) Pol ι (400 nM) and (**F**) Pol η (400 nM). Only Pol ζ and Rev1 preferentially inserted the right dCMP opposite the CP ICL.

analyzed how the polymerases interacted with the less distorting NML ICLs: the hydrazine ICL (HY ICL), which introduces a ~15° bend in the DNA while retaining mostly B-form DNA (Figure 1B) and the dimethylethylenediamine ICL (DA ICL), which is expected to be free of any helix distortion (Figure 1C). The HY1 and DA1 substrates, in which the ICL is part of a 20-mer duplex, and the HY2 and DA2 substrates, in which the duplex portion around the ICL is shortened to six nucleotides, were annealed to the P14/15 and P6/7 primers, respectively, and incubated with the various TLS polymerases.

Pol ζ stalled 1 and 3 nt before the insertion opposite to the adducted guanine on HY1 and DA1 templates, respectively (Figure 5A, lanes 1–3 and 7–9), similar to what we observed with the CP1 substrate, although the initial strand displacement reaction was slower for the DA1 substrate. Interestingly, there was a marked difference in how Pol ζ reacted with the resected HY2 and DA2 substrates. The extension reaction was completely blocked at −1 position with HY ICL (Figure 5A, lane 6), leading to an even lower degree of insertion and bypass than with CP ICL. On the other hand, Pol ζ was able to bypass the DA ICL on the DA2 substrate with a yield of about 16% of full-length product (Figure 5A, lane 12), suggesting that increasing the length of the linker between the guanines greatly facilitated bypass by Pol ζ. Conversely, initial strand displacement was inhibited to a greater extent in the more stable DA duplexes.
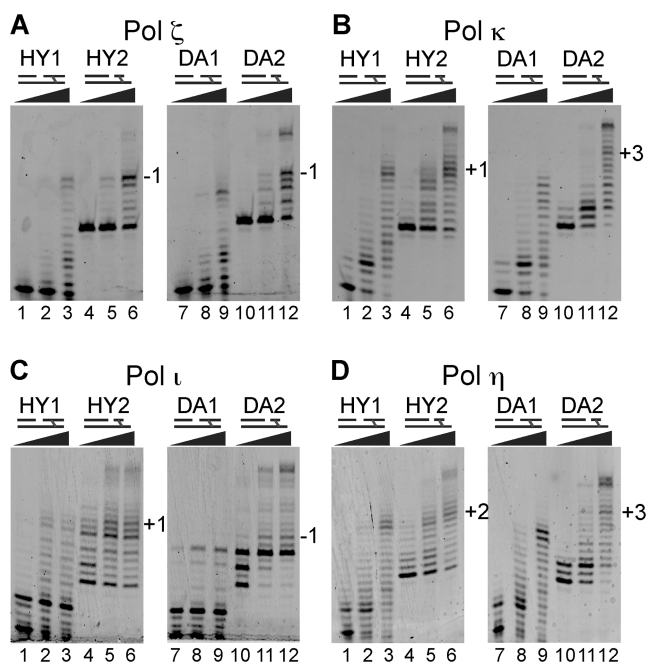

Figure 5. Resected NML ICLs can be bypassed by multiple Y-family polymerases. Full-length (HY1, DA1) and 5′- and 3′-resected (HY2, DA2) NML templates were annealed to primers P15 and P7, respectively, and incubated with increasing concentrations of (**A**) Pol ζ (0.4, 4, 35 nM), (**B**) Pol κ (0.2, 2, 20 nM), (**C**) Pol ι (4, 40, 400 nM) and (**D**) Pol η (4, 40, 400 nM). The position of the main stalling points is indicated at the right side of the gels. Note the marked presence of full length products indicated.

The Y-family polymerases were more efficient in bypassing NML ICLs than CP ICL and resection of the dsDNA portion around the ICL markedly facilitated the approach, insertion and bypass of the HY and DA ICLs. Thus, Pol κ had pausing sites on the HY2 template at 0, +1 and +2 positions, but was able to fully extend 12% of the HY2 templates (Figure 5B, lane 6). The bypass of the lesion in DA2 template was even more efficient (25% full-length product) and proceeded without any pronounced pausing sites at the ICL, indicating that the DA ICL in a 6-mer duplex does not prevent insertion and bypass by Pol κ (Figure 5B, compare lanes 9 and 12). Interestingly, initial strand displacement was inhibited to a greater extent by the DA than the HY ICL (Figure 5B, compare lane 5 with lane 11). It, therefore, appears that helical distortion by the ICL facilitates strand displacement, while increased length of the ICL facilitates bypass.

Similar results were observed with Pol ι, which bypassed the HY and DA ICLs, yielding 12 and 31% full-length product, respectively, and was only slowed down on the HY2 template with pausing sites at −1, 0 and +1 positions (Figure 5C, lanes 1–6). For the DA2 substrate strand, displacement was a bigger obstacle than for the HY2 substrate and 60% of the primer stalled at the start of duplex DNA and at −3 position (Figure 5C, lane 10). This reinforces the notion that the more stable duplex structure of the DA ICL can inhibit the strand displacement reaction.

Pol η was the most efficient Y-family polymerase in bypassing the NML ICLs. It was even able to bypass efficiently the fully double-stranded substrate HY1 stalling at the +2 position (Figure 5D, lane 3). On the resected HY2 substrate, Pol η was also only slowed down with pausing site at +1, +2 and +3 positions (making up 9, 17 and 10% of the products, respectively, Figure 5D, lane 6). In contrast, Pol η was barely able to approach the DA ICL in the DA1 template stalling at −1 position (Figure 5D, lane 9). However, Pol η efficiently bypassed the resected DA2 substrate. Again, pausing sites at the beginning of the crosslinked strand were observed, which were specific for the DA ICL (Figure 5D, lanes 5 and 11). But once the strand is displaced, Pol η was able to extend to the end with no additional major pausing sites with a pattern similar to Pol κ yielding 37% of full-length product (compare Figure 5B and C, lane 12).

Single-nucleotide insertions opposite NML ICLs

Analogous to the CP4 substrate, we carried out single nucleotide insertion studies using the HY2 and DA2 substrates annealed to the NMP1 primer (Figure 1D), to study the accuracy of the insertion opposite the NML ICLs. As seen before, the insertion at the HY ICL by Pol ζ was very inefficient (Figure 6A), and the insertion was specific for dCMP, incorporating 2 nt opposite the two consecutive guanosines. In contrast, insertion by Pol ζ opposite a DA ICL was comparable to CP ICL and was also specific for dCMP, suggesting that the structure of DA ICL is more accessible than the HY ICL for Pol ζ (Figure 6A). Rev1 was unable to perform any insertion opposite either of the two NML ICLs (Figure 6B) and also
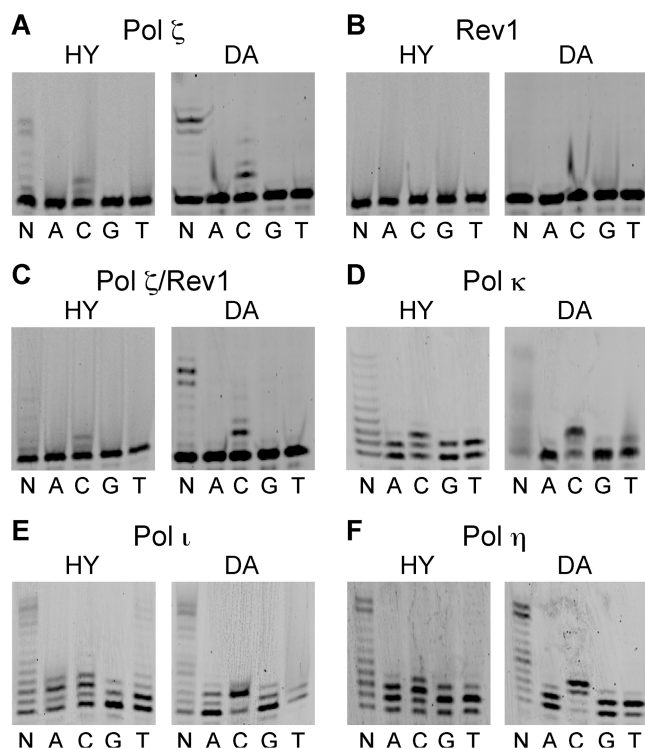
Figure 6. Partially accurate bypass of the non-disorting DA ICLs. The HY2 and DA2 templates were annealed to the NMP1 primer and incubated with the indicated dNTPs and (**A**) Pol ζ (35 nM), (**B**) Rev1 (40 nM), (**C**) Pol ζ/Rev1 (20 nM), (**D**) Pol κ (20 nM), (**E**) Pol ι (400 nM) and (**F**) Pol η (400 nM). Insertion of dCTP by Pol ζ opposite to DA ICL was more efficient than insertion opposite to the HY ICL, and a slight preference for correct dCTP insertion can be observed with the longer DA ICL for Pol κ, ι and η.

failed to stimulate Pol ζ (Figure 6C), reiterating the observation that Pol ζ and Rev1 do not optimally work together in this experimental setup.

Pol κ inserted any dNTP opposite the HY ICL, but the incorporation of a nucleotide opposite the G following the adduct was selective for dCMP (Figure 6C). On the other hand, dCMP insertion was preferentially catalyzed by Pol κ opposite the DA ICL, indicating that the longer linker allows Pol κ to insert the correct base.

The insertion reaction opposite the crosslinked G in HY ICL with Pol ι showed that any of the dNTPs were inserted, with dGMP being the least efficient (Figure 6E). Additionally, the insertion product was efficiently extended by one and two nucleotides in presence of dATP and dCTP, respectively. In case of the DA ICL, Pol ι had a clear preference for dCMP and incorporated dCMP at 0 and +1 positions.

Insertion by Pol η was highly inaccurate for both NML ICLs and any of the dNTPs were incorporated (Figure 6, Pol η). However, extension from the insertion product with a dNTP other than dCMP was more prominent with HY ICL than with the DA ICL. As seen before with Pol κ and Pol ι, the extension reactions are more accurate for DA ICLs than for HY ICLs and occurred almost exclusively in the presence of dCTP.

DISCUSSION

TLS is an essential step in the repair of ICLs. Current models of replication-dependent and -independent ICL repair suggest that following recognition of the ICL, incisions are made in its vicinity and followed by TLS past the unhooked ICL leading to restoration of one of the DNA strands (Supplementary Figure S1). This intact strand may then serve as a template to complete the repair by excision repair or HR (4,50). Among at least 15 mammalian DNA polymerases, Pol ζ and Rev1 appear to be the most important ones for ICL repair based on genetic considerations (11,17,51,52). Moreover, the activity of Pol ζ was recently shown to be necessary for replication-dependent repair of a defined CP ICL in *Xenopus laevis* egg extracts (14).

There is increasing evidence, however, that additional DNA polymerases are involved in ICL repair. Pol κ has been shown to bypass minor groove ICLs *in vitro* and cells deficient in Pol κ are sensitive to agents that form ICLs in the minor groove (27). Pol ν on the other hand can bypass ICLs formed in the major groove, but not those formed in the minor groove (28). More indirect evidence has implicated Pol η in ICL repair (23–25,53). Based on these observations, we undertook a systematic analysis of the role of various TLS polymerases in bypassing major groove ICLs, taking advantage of our ability to generate site-specific ICLs that induce different degrees of distortion (29,30).

Truncation of the DNA around the ICL facilitates TLS

Our results suggest that two factors facilitate the bypass of ICLs by polymerases: the resection of the crosslinked non-template strand and the length of the bridge of the ICL. As shown previously for Pol κ and Pol ν (27,28), resection of the non-replicated crosslinked strand to a few nucleotides markedly facilitates advancement of polymerases to the ICL regardless of the position of the ICL. Resection of the dsDNA on both sides of the ICL allowed for the bypass of at least some ICLs used in our studies by Pol ζ, Pol η, Pol ι and Pol κ (Figures 3 and 5), indicating that strand displacement is a major limiting factor for the TLS of ICLs.

These observations raise the question in what state of resection the TLS machinery encounters ICLs during repair in cells. While we do not presently know the answer to this question, it is likely that TLS of ICLs is preceded by two incisions of the non-template strand on either side of the ICL (50,54). The positions of these incision sites are presently unknown, but it is very possible that they occur very close to the ICL, since at least in replication-dependent ICL repair, the replication fork can approach to the position immediately before the ICL, before any incisions take place (54). Furthermore, at least one exonuclease with 5′ to 3′ polarity, SNM1 (55,56) has been implicated in ICL repair and the resection of incised ICLs in replication-independent ICL repair (13,57). Regardless of how the resected ICLs arise, it is plausible that the dsDNA around the ICL is processed to a structure containing a few nucleotides of dsDNA around the ICL. In fact, it has been shown that one of the

products formed during replication-dependent ICL repair in xenopus egg extracts contained an ICL consisting of a single nucleotide (14). The substrates may therefore be realistic mimics of what TLS polymerases may encounter under physiological conditions.

Longer and more flexible ICLs are more easily bypassed by TLS polymerases

Our studies revealed that the length of the ICL bridge connecting the N7 positions of guanine bases on opposing strands has a big influence on the ability of TLS polymerases to bypass ICLs. The distance of the two crosslinked guanosine bases in our studies ranged from 2.8 Å for the CP ICL to 6.8 Å for nitrogen mustard mimic HY ICL to an estimated 8.9 Å for the DA ICL, resulting in severe, minor or no distortion of the DNA duplex (Figure 1). Two distinct effects of the degree of distortion induced by the ICL were observed: first, more distorting ICLs make it easier for polymerases to approach the ICL, presumably because the distortion destabilizes the DNA duplex and facilitates strand displacement synthesis. Second, and more importantly, lesion bypass and extension past the lesion occur more readily with ICLs with a longer bridge. We rationalize this observation with the increased flexibility of the two crosslinked bases. After appropriate resection of the ICL, these major groove ICLs could be considered to be very bulky major groove lesion that can be accommodated in the active site of TLS polymerases. It is worth noting that our studies were carried out using high enzyme to template ratios, and may therefore not really represent physiological conditions. However, since our studies were carried out in the absence of accessory factors such as PCNA, we believe that they reveal the intrinsic capabilities of TLS DNA polymerases in bypassing ICLs. More detailed kinetic investigations as well as studies that include accessory factors such as PCNA will be required to determine the optimal conditions for ICL bypass by various DNA polymerases.

Structural studies of TLS polymerases provide some indication as to why Pol η might be particularly well suited to mediate the bypass of ICLs with flexible bridges. Snapshots of different steps of Pol η bypassing cyclopyrimidine dimer (CPD) adducts revealed that this enzyme has a larger active site than other TLS polymerases (58,59). Additionally, Pol η binds rigidly to five residues of a template/primer duplex ensuring that the CPDs, which deform the DNA, are forced in a B-form type duplex in the enzyme active site. While all TLS polymerases have a more open active site than replicative polymerases, these features of Pol η might be particularly suitable to bypass ICLs by accommodating them in the enlarged active site and reducing interference from the third strand by tightly binding template and primer strand in the active site. Pol κ encircles the DNA with its N-clasp domain, and this might provide a firm grip on the duplex DNA in the presence of a third strand (60). The major groove in vicinity of the template base is solvent accessible, but the opening is rather narrow and would likely pose a problem to accommodate the third

strand of an ICL substrate. This might explain why Pol κ is unable to insert a dNTP opposite a CP ICL, while it has the ability to do so opposite more relaxed HY and DA ICLs. In contrast, we have no satisfactory structural explanation for how Pol ι might be able to bypass ICLs, since structural studies have shown that this enzyme rotates the template base into the syn conformation and uses a Hoogsteen base pair to incorporate a dNTP opposite a lesion (61).

Recent studies of replication-dependent ICL repair in *Xenopus laevis* oocyte extracts also show that the structure of ICLs can influence which TLS polymerase is used in the bypass step. In this system, the replication-dependent repair of ICL can be observed in step-by-step fashion and the following steps have been discerned (14): stalling of a pair of replication forks at some distance (20–40 nt) on either side of the ICL, approach of one of the forks to the −1 position before the ICL, incision of the non-template strand and insertion of a dNTP opposite the ICL, extension and complete extension of one of the two strands. The repair of CP ICLs was dramatically reduced in cells depleted of the Rev7 subunit of Polζ, while the repair of the DA ICLs occurred normally. These observations demonstrate that multiple TLS polymerases can contribute to ICL repair and the structure of the ICL is one of the factors influencing polymerase choice.

Regulation of TLS in ICL repair

Our results provide insight into the basic biochemical properties and structural requirements of TLS polymerases in bypassing ICLs. It is obvious, however, that the activity of these enzymes in a cellular context is regulated through interactions with other proteins in a specific temporal and spatial context (50). As discussed above, genetic and cellular studies clearly indicate that Pol ζ and Rev1 have a key role in mediating TLS of ICLs, yet these two enzymes were less efficient in the bypass of ICLs than the Y-family polymerases Pol η, Pol ι and Pol κ (Figures 3 and 5). While it is possible that this is in part due to the enzyme preparations used in our study, it more likely reflects the need for a more physiological environment. Studies have shown that the activity of Pol ζ in bypassing UV-damaged DNA is greatly stimulated by interaction with PCNA *in vitro* (62,63). *In vivo*, it has been shown that replication-independent ICL repair depends on the interaction of ubiquitinated PCNA and Pol ζ (12,13). While the bypass of lesions affecting one strand of DNA is principally regulated through interaction with ubiquitinated PCNA (8,64), TLS polymerases appear to be recruited to sites of the main replication-dependent ICL repair pathway in a distinct manner. Replication-dependent ICL repair depends on the activation of the Fanconi anemia pathway and involves the monoubiquitination of the FancD2-FancI proteins by the multisubunit core complex possibly in conjunction with ubiquitnated PCNA (4,65). Recent studies have shown that FA pathway is directly involved in ICL repair by facilitating the TLS and/or incision steps (54). Based on the analogy with ubiquitinated PCNA, it is

therefore, likely that the interaction of TLS polymerases with monoubiquitinated FancD2-FancI is key to regulating TLS activity in replication-dependent ICL repair. Future studies will aim to elucidate how the intrinsic biochemical activities of TLS polymerases revealed in the current study together with regulatory elements determine the choice of polymerase in the repair of ICLs.

SUPPLEMENTARY DATA

Supplementary Data are available at NAR Online.

ACKNOWLEDGEMENTS

FUNDING

REFERENCES

1. Schärer,O.D. (2005) DNA interstrand crosslinks: natural and drug-induced DNA adducts that induce unique cellular responses. *Chembiochem*, **6**, 27–32.
2. Noll,D.M., Mason,T.M. and Miller,P.S. (2006) Formation and Repair of Interstrand Cross-Links in DNA. *Chem. Rev.*, **106**, 277–301.
3. Stone,M.P., Cho,Y.J., Huang,H., Kim,H.Y., Kozekov,I.D., Kozekova,A., Wang,H., Minko,I.G., Lloyd,R.S., Harris,T.M. *et al.* (2008) Interstrand DNA cross-links induced by alpha,beta-unsaturated aldehydes derived from lipid peroxidation and environmental sources. *Acc. Chem. Res.*, **41**, 793–804.
4. Moldovan,G. and D'Andrea,A. (2009) How the Fanconi Anemia Pathway Guards the Genome. *Annu. Rev. Genet.*, **43**, 223–249.
5. Muniandy,P.A., Liu,J., Majumdar,A., Liu,S.T. and Seidman,M.M. (2009) DNA interstrand crosslink repair in mammalian cells: step by step. *Crit. Rev. Biochem. Mol. Biol.*, **45**, 23–49.
6. Guainazzi,A. and Schärer,O.D. (2010) Using synthetic DNA interstrand crosslinks to elucidate repair pathways and identify new therapeutic targets for cancer chemotherapy. *Cell. Mol. Life Sci.*, **67**, 3683–3697.
7. McCulloch,S.D. and Kunkel,T.A. (2008) The fidelity of DNA synthesis by eukaryotic replicative and translesion synthesis polymerases. *Cell Res.*, **18**, 148–161.
8. Waters,L.S., Minesinger,B.K., Wiltrout,M.E., D'Souza,S., Woodruff,R.V. and Walker,G.C. (2009) Eukaryotic translesion polymerases and their roles and regulation in DNA damage tolerance. *Microbiol. Mol. Biol. Rev.*, **73**, 134–154.
9. Sonoda,E., Okada,T., Zhao,G.Y., Tateishi,S., Araki,K., Yamaizumi,M., Yagi,T., Verkaik,N.S., van Gent,D.C., Takata,M. *et al.* (2003) Multiple roles of Rev3, the catalytic subunit of polzeta in maintaining genome stability in vertebrates. *EMBO J.*, **22**, 3188–3197.
10. Wu,H.I., Brown,J.A., Dorie,M.J., Lazzeroni,L. and Brown,J.M. (2004) Genome-wide identification of genes conferring resistance
to the anticancer agents cisplatin, oxaliplatin and mitomycin C. *Cancer Res.*, **64**, 3940–3948.
11. Nojima,K., Hochegger,H., Saberi,A., Fukushima,T., Kikuchi,K., Yoshimura,M., Orelli,B.J., Bishop,D.K., Hirano,S., Ohzeki,M. *et al.* (2005) Multiple repair pathways mediate tolerance to chemotherapeutic cross-linking agents in vertebrate cells. *Cancer Res.*, **65**, 11704–11711.
12. Shen,X., Jun,S., O'Neal,L.E., Sonoda,E., Bemark,M., Sale,J.E. and Li,L. (2006) REV3 and REV1 Play Major Roles in Recombination-independent Repair of DNA Interstrand Cross-links Mediated by Monoubiquitinated Proliferating Cell Nuclear Antigen (PCNA). *J. Biol. Chem.*, **281**, 13869–13872.
13. Sarkar,S., Davies,A.A., Ulrich,H.D. and McHugh,P.J. (2006) DNA interstrand crosslink repair during G1 involves nucleotide excision repair and DNA polymerase zeta. *EMBO J.*, **25**, 1285–1294.
14. Räschle,M., Knipscheer,P., Enoiu,M., Angelov,T., Sun,J., Griffith,J.D., Ellenberger,T.E., Schärer,O.D. and Walter,J.C. (2008) Mechanism of replication-coupled DNA interstrand crosslink repair. *Cell*, **134**, 969–980.
15. Prakash,S., Johnson,R.E. and Prakash,L. (2005) Eukaryotic translesion synthesis DNA polymerases: specificity of structure and function. *Annu. Rev. Biochem.*, **74**, 317–353.
16. Gan,G.N., Wittschieben,J.P., Wittschieben,B.Ø. and Wood,R.D. (2008) DNA polymerase zeta (pol zeta) in higher eukaryotes. *Cell Res.*, **18**, 174–183.
17. Simpson,L.J. and Sale,J.E. (2003) Rev1 is essential for DNA damage tolerance and non-templated immunoglobulin gene mutation in a vertebrate cell line. *EMBO J.*, **22**, 1654–1664.
18. Niedzwiedz,W., Mosedale,G., Johnson,M., Ong,C.Y., Pace,P. and Patel,K.J. (2004) The Fanconi anaemia gene FANCC promotes homologous recombination and error-prone DNA repair. *Mol. Cell*, **15**, 607–620.
19. Nelson,J.R., Lawrence,C.W. and Hinkle,D.C. (1996) Deoxycytidyl transferase activity of yeast REV1 protein. *Nature*, **382**, 729–731.
20. Lin,W., Xin,H., Zhang,Y., Wu,X., Yuan,F. and Wang,Z. (1999) The human REV1 gene codes for a DNA template-dependent dCMP transferase. *Nucleic Acids Res.*, **27**, 4468–4475.
21. Haracska,L., Prakash,S. and Prakash,L. (2002) Yeast Rev1 protein is a G template-specific DNA polymerase. *J. Biol. Chem.*, **277**, 15546–15551.
22. Washington,M.T., Minko,I.G., Johnson,R.E., Haracska,L., Harris,T.M., Lloyd,R.S., Prakash,S. and Prakash,L. (2004) Efficient and error-free replication past a minor-groove N2-guanine adduct by the sequential action of yeast Rev1 and DNA polymerase zeta. *Mol. Cell. Biol.*, **24**, 6900–6906.
23. Misra,R.R. and Vos,J.M. (1993) Defective replication of psoralen adducts detected at the gene-specific level in xeroderma pigmentosum variant cells. *Mol. Cell. Biol.*, **13**, 1002–1012.
24. Albertella,M.R., Green,C.M., Lehmann,A.R. and O'Connor,M.J. (2005) A role for polymerase eta in the cellular tolerance to cisplatin-induced damage. *Cancer Res.*, **65**, 9799–9806.
25. Chen,Y.-w., Cleaver,J.E., Hanaoka,F., Chang,C.-f. and Chou,K.-m. (2006) A novel role of DNA polymerase eta in modulating cellular sensitivity to chemotherapeutic agents. *Mol. Cancer Res.*, **4**, 257–265.
26. Zheng,H.Y., Wang,X., Warren,A.J., Legerski,R.J., Nairn,R.S., Hamilton,J.W. and Li,L. (2003) *Mol. Cell. Biol.*, **23**, 754–761.
27. Minko,I.G., Harbut,M.B., Kozekov,I.D., Kozekova,A., Jakobs,P.M., Olson,S.B., Moses,R.E., Harris,T.M., Rizzo,C.J. and Lloyd,R.S. (2008) Role for DNA polymerase kappa in the processing of N2-N2-guanine interstrand crosslinks. *J. Biol. Chem.*, **283**, 17075–17082.
28. Yamanaka,K., Minko,I.G., Takata,K., Kolbanovskiy,A., Kozekov,I.D., Wood,R.D., Rizzo,C.J. and Lloyd,R.S. (2010) Novel enzymatic function of DNA polymerase nu in translesion DNA synthesis past major groove DNA-peptide and DNA-DNA cross-links. *Chem. Res. Toxicol.*, **23**, 689–695.
29. Angelov,T., Guainazzi,A. and Schärer,O.D. (2009) Generation of DNA interstrand cross-links by post-synthetic reductive amination. *Org. Lett.*, **11**, 661–664.
30. Guainazzi,A., Campbell,A.J., Angelov,T., Simmerling,C. and Schärer,O.D. (2010) Synthesis and molecular modeling of a

nitrogen mustard DNA interstrand crosslink. *Chem. Eur. J.*, **16**, 12100–12103.

31. Hofr,C. and Brabec,V. (2001) Thermal and thermodynamic properties of duplex DNA containing site-specific interstrand cross-link of antitumor cisplatin or its clinically ineffective trans isomer. *J. Biol. Chem.*, **276**, 9655–9661.

32. Frank,E.G. and Woodgate,R. (2007) Increased catalytic activity and altered fidelity of human DNA polymerase iota in the presence of manganese. *J. Biol. Chem.*, **282**, 24689–24696.

33. Zhang,Y., Yuan,F., Xin,H., Wu,X., Rajpal,D.K., Yang,D. and Wang,Z. (2000) Human DNA polymerase kappa synthesizes DNA with extraordinarily low fidelity. *Nucleic Acids Res.*, **28**, 4147–4156.

34. Guo,D., Wu,X., Rajpal,D.K., Taylor,J.S. and Wang,Z. (2001) Translesion synthesis by yeast DNA polymerase zeta from templates containing lesions of ultraviolet radiation and acetylaminofluorene. *Nucleic Acids Res.*, **29**, 2875–2883.

35. Lemaire,M.A., Schwartz,A., Rahmouni,A.R. and Leng,M. (1991) Interstrand cross-links are preferentially formed at the d(GC) sites in the reaction between cis-diamminedichloroplatinum (II) and DNA. *Proc. Natl Acad. Sci. USA*, **88**, 1982–1985.

36. Ojwang,J.O., Grueneberg,D.A. and Loechler,E.L. (1989) Synthesis of a duplex oligonucleotide containing a nitrogen mustard interstrand DNA-DNA cross-link. *Cancer Res.*, **49**, 6529–6537.

37. Millard,J., Raucher,S. and Hopkins,P. (1990) Mechlorethamine Cross-Links Deoxy guanosine Residues at 5′-GNC Sequences in Duplex DNA Fragments. *J. Am. Chem. Soc.*, **112**, 2459–2460.

38. Rink,S.M., Solomon,M.S., Taylor,M.J., Rajur,S.B., McLaughlin,L.W. and Hopkins,P.B. (1993) Covalent Structure of a Nitrogen Mustard-Induced DNA Interstrand Cross-Link: An N7-to-N7 Linkage of Deoxyguanosine Residues at theDuplex Sequence 5′-d(GNC). *J. Am. Chem. Soc.*, **115**, 2551–2557.

39. Huang,H., Zhu,L., Reid,B.R., Drobny,G.P. and Hopkins,P.B. (1995) Solution Structure of a Cisplatin-Induced DNA Interstrand Cross-Link. *Science*, **270**, 1842–1845.

40. Coste,F., Malinge,J.-M., Serre,L., Shepard,W., Roth,M., Leng,M. and Zelwer,C. (1999) Crystal structure of a double-stranded DNA containing a cisplatin interstrand cross-link at 1.63 Å resolution: hydration at the platinated site. *Nucleic Acids Res.*, **27**, 1837–1846.

41. Rink,S.M. and Hopkins,P.B. (1995) A mechlorethamine-induced DNA interstrand cross-link bends duplex DNA. *Biochemistry*, **34**, 1439–1445.

42. Nelson,J.R., Lawrence,C.W. and Hinkle,D.C. (1996) Thymine-thymine dimer bypass by yeast DNA polymerase zeta. *Science*, **272**, 1646–1649.

43. Guo,C., Fischhaber,P.L., Luk-Paszyc,M.J., Masuda,Y., Zhou,J., Kamiya,K., Kisker,C. and Friedberg,E.C. (2003) Mouse Rev1 protein interacts with multiple DNA polymerases involved in translesion DNA synthesis. *EMBO J.*, **22**, 6621–6630.

44. Haracska,L., Unk,I., Johnson,R.E., Johansson,E., Burgers,P.M., Prakash,S. and Prakash,L. (2001) Roles of yeast DNA polymerases delta and zeta and of Rev1 in the bypass of abasic sites. *Genes Dev.*, **15**, 945–954.

45. Nair,D.T., Johnson,R.E., Prakash,L., Prakash,S. and Aggarwal,A.K. (2005) Rev1 employs a novel mechanism of DNA synthesis using a protein template. *Science*, **309**, 2219–2222.

46. Ohashi,E., Ogi,T., Kusumoto,R., Iwai,S., Masutani,C., Hanaoka,F. and Ohmori,H. (2000) Error-prone bypass of certain DNA lesions by the human DNA polymerase kappa. *Genes Dev.*, **14**, 1589–1594.

47. Tissier,A., McDonald,J.P., Frank,E.G. and Woodgate,R. (2000) poliota, a remarkably error-prone human DNA polymerase. *Genes Dev.*, **14**, 1642–1650.

48. Zhang,Y., Yuan,F., Wu,X., Wang,M., Rechkoblit,O., Taylor,J.S., Geacintov,N.E. and Wang,Z. (2000) Error-free and error-prone lesion bypass by human DNA polymerase kappa *in vitro*. *Nucleic Acids Res.*, **28**, 4138–4146.

49. Ohashi,E., Bebenek,K., Matsuda,T., Feaver,W.J., Gerlach,V.L., Friedberg,E.C., Ohmori,H. and Kunkel,T.A. (2000) Fidelity and processivity of DNA synthesis by DNA polymerase kappa, the product of the human DINB1 gene. *J. Biol. Chem.*, **275**, 39678–39684.

50. Ho,T.V. and Schärer,O.D. (2010) Translesion DNA synthesis polymerases in DNA interstrand crosslink repair. *Environ. Mol. Mutagen.*, **51**, 552–566.

51. Wu,F., Lin,X., Okuda,T. and Howell,S.B. (2004) DNA polymerase zeta regulates cisplatin cytotoxicity, mutagenicity and the rate of development of cisplatin resistance. *Cancer Res.*, **64**, 8029–8035.

52. Wittschieben,J.P., Reshmi,S.C., Gollin,S.M. and Wood,R.D. (2006) Loss of DNA polymerase zeta causes chromosomal instability in mammalian cells. *Cancer Res.*, **66**, 134–142.

53. Mogi,S., Butcher,C.E. and Oh,D.H. (2007) DNA polymerase eta reduces the gamma-H2AX response to psoralen interstrand crosslinks in human cells. *Exp. Cell. Res.*, **314**, 887–895.

54. Knipscheer,P., Räschle,M., Smogorzewska,A., Enoiu,M., Ho,T.V., Schärer,O.D., Elledge,S.J. and Walter,J.C. (2009) The Fanconi Anemia Pathway Promotes Replication-Dependent DNA Interstrand Cross-Link Repair. *Science*, **326**, 1698–1701.

55. Li,X., Hejna,J. and Moses,R.E. (2005) The yeast Snm1 protein is a DNA 5′-exonuclease. *DNA Repair*, **4**, 163–170.

56. Hejna,J., Philip,S., Ott,J., Faulkner,C. and Moses,R. (2007) The hSNM1 protein is a DNA 5′-exonuclease. *Nucleic Acids Res.*, **35**, 6115–6123.

57. Cattell,E., Sengerova,B. and McHugh,P.J. (2010) The SNM1/Pso2 family of ICL repair nucleases: from yeast to man. *Environ. Mol. Mutagen.*, **51**, 635–645.

58. Biertumpfel,C., Zhao,Y., Kondo,Y., Ramon-Maiques,S., Gregory,M., Lee,J.Y., Masutani,C., Lehmann,A.R., Hanaoka,F. and Yang,W. (2010) Structure and mechanism of human DNA polymerase eta. *Nature*, **465**, 1044–1048.

59. Silverstein,T.D., Johnson,R.E., Jain,R., Prakash,L., Prakash,S. and Aggarwal,A.K. (2010) Structural basis for the suppression of skin cancers by DNA polymerase eta. *Nature*, **465**, 1039–1043.

60. Lone,S., Townson,S.A., Uljon,S.N., Johnson,R.E., Brahma,A., Nair,D.T., Prakash,S., Prakash,L. and Aggarwal,A.K. (2007) Human DNA polymerase kappa encircles DNA: implications for mismatch extension and lesion bypass. *Mol. Cell*, **25**, 601–614.

61. Nair,D.T., Johnson,R.E., Prakash,S., Prakash,L. and Aggarwal,A.K. (2004) Replication by human DNA polymerase-iota occurs by Hoogsteen base-pairing. *Nature*, **430**, 377–380.

62. Garg,P., Stith,C.M., Majka,J. and Burgers,P.M. (2005) Proliferating cell nuclear antigen promotes translesion synthesis by DNA polymerase zeta. *J. Biol. Chem.*, **280**, 23446–23450.

63. Wood,A., Garg,P. and Burgers,P.M. (2007) A ubiquitin-binding motif in the translesion DNA polymerase Rev1 mediates its essential functional interaction with ubiquitinated proliferating cell nuclear antigen in response to DNA damage. *J. Biol. Chem.*, **282**, 20256–20263.

64. Jansen,J.G., Fousteri,M.I. and de Wind,N. (2007) Send in the clamps: control of DNA translesion synthesis in eukaryotes. *Mol. Cell*, **28**, 522–529.

65. Geng,L., Huntoon,C.J. and Karnitz,L.M. (2010) RAD18-mediated ubiquitination of PCNA activates the Fanconi anemia DNA repair network. *J. Cell. Biol.*, **191**, 249–257.